공학석사 학위논문

Preparation of a hydrogel-based SPR sensor for detection of antibody/antigen interactions

항체/항원 상호작용을 감지하는 하이드로겔 기반 SPR 센서 합성

2021 년 2 월

서울대학교 대학원

화학생물공학부

Jie Ying Teoh

항체/항원 상호작용을 감지하는 하이드로겔 기반 SPR 센서 합성

지도교수 유동원

이 논문을 공학석사 학위논문으로 제출함

2021 년 2 월

서울대학교 대학원

화학생물공학부

Jie Ying Teoh

Jie Ying Teoh의 석사 학위논문을 인준함

2021 년 2 월

위 원 장 김 영 유 (인)

부 위 원 장 유 동 원 (인)

위 원 오 준 학 (인)

Abstract

Preparation of a hydrogel-based SPR sensor for detection of antibody/antigen interactions

Jie Ying Teoh

Department of Chemical and Biological Engineering

The Graduate School

Seoul National University

SPR biosensors are often used for the detection and diagnosis of biomolecular interactions as they allow monitoring of these interactions in real-time, without the need for pre-labelling. However, these SPR biosensors suffer from several limitations such as inability to distinguish between nonspecific and specific interactions and low sensitivities.

The sensor chip is one of the most important components of the SPR biosensor and the properties of the sensor chip govern the sensitivity and specificity of the sensor in presence of analyte. Since bioresponsive hydrogels have been reported to have antifouling properties, along with selectivity for specific stimuli, grafting of hydrogels can be expected to improve the specificity of the SPR biosensor. The three-dimensional structure of the gel matrix also provides more attachment sites for ligand immobilization, which can improve the sensitivity of the biosensor.

In this work, bioresponsive SPR sensor chips were fabricated from surface modification of bare gold sensor chips with bioresponsive hydrogels. The facile synthesis of hydrogels allowed us to prepare a library of hydrogels with different physical properties. The effect of the physical properties of the hydrogel on the SPR response was then examined. Our results demonstrate the potential of engineering hydrogel properties to produce SPR biosensors of optimal sensitivity in different concentration ranges.

Keyword: hydrogels, antibody/antigen interactions, protein multivalent binding (PMB), surface plasmon resonance, biosensor

Student Number: 2019-25979

Table of Contents

List of Figures

List of Tables

List of Acronyms

AAc	Acrylic acid
APS	Ammonium persulfate
BIS	*N*,*N'*-methylenebisacrylamide
D_h	Hydrodynamic diameter
DLS	Dynamic light scattering
EDC	1-Ethyl-3-(3-dimethylaminopropyl)carbodiimide
MES	2-(*N*-Morpholino)ethanesulfonic acid
NHS	*N*-hydroxysuccinimide
NIPAM	*N*-isopropylacrylamide
PDI	Polydispersity index
PMB	Protein multivalent binding
R_h	Hydrodynamic radius
RI	Refractive index
RUmax	Maximum resonance unit
SDS	Sodium dodecyl sulfate
SNR	Signal to noise ratio
SPR	Surface plasmon resonance
Tween 80	Poly(oxyethylene)sorbitan monooleate

Chapter 1. Introduction

1.1 Surface plasmon resonance biosensors

Surface plasmon resonance (SPR) biosensors are optical sensors widely used for detection of biomolecular interactions and determination of their kinetics. SPR sensors provide insight into affinities of interactions between ligands and their targets without the need to label the biomolecule, which is important as labelling materials may occupy important binding sites or cause steric hindrance.[1] Binding events can also be monitored in real time by establishing the time course of the SPR response.[2]

Surface plasmons (SPs) are longitudinal electromagnetic waves propagating along the interface between a metal and dielectric medium.[3] These SPs are excited when the magnitude of the parallel component of the wave vector of incident light (k_x) matches that of the wave vector of the SPs (k_{sp}). k_x and k_{sp} are expressed as follows:

$$k_{sp} = k_0\sqrt{\frac{\varepsilon_m(\lambda).\varepsilon_s(\lambda)}{\varepsilon_m(\lambda)+\varepsilon_s(\lambda)}} = \frac{2\pi}{\lambda}\sqrt{\frac{\varepsilon_m(\lambda).\varepsilon_s(\lambda)}{\varepsilon_m(\lambda)+\varepsilon_s(\lambda)}} \qquad (1)$$

$$k_x = k_0\sqrt{\varepsilon_d}\sin(\theta) = \frac{2\pi}{\lambda}\sqrt{\varepsilon_d}\sin(\theta) \qquad (2)$$

The coupling of SPs and the evanescent wave of the incident light occurs at a specific incident angle known as the SPR angle (θ_{SPR}), as illustrated in

Figure 1a. At θ_{SPR}, a minimum in the reflected light intensity is observed due to the transfer of energy from the light wave to SPs.

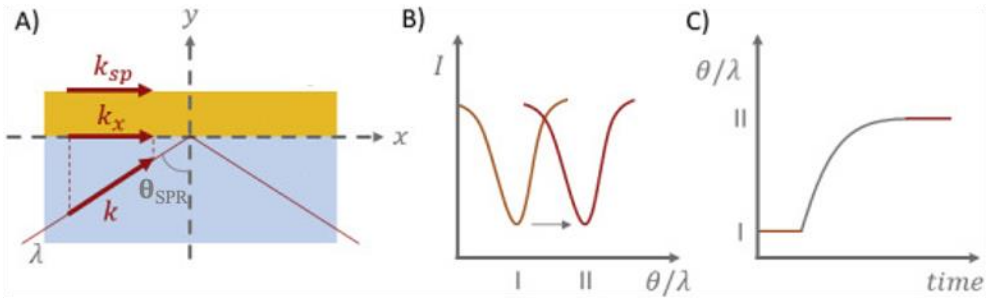

Figure 1. (a) Coupling of the parallel component of the light wave (k_x) with the wave vector of the SPs (k_{sp}) at the SPR angle (θ_{SPR}) leads to surface plasmon resonance on a metal/dielectric interface. (b) Change in the RI of the surrounding medium causes a change in θ_{SPR}. (c) The change in θ_{SPR} can be plotted against time to give a sensorgram. Figure was adapted from reference.[4]

Adsorption of molecules on the metal surface causes changes in the refractive index (RI) and dielectric constant of the surrounding medium (ε_S), which then changes the k_{sp}. This in turn changes k_x and θ_{SPR}.[4] SPR sensors detect the shift in θ_{SPR} (Figure 1b) and the change of θ_{SPR} with time is given by the sensorgram (Figure 1c).[5,6] Binding affinities, kinetic information and amount of analyte bound to the sensor chip can be obtained easily through the sensorgram.[7]

In a typical analysis cycle, the sensor chip surfaces are first conditioned with buffer solution to obtain the baseline, given as point I in Figure 1c. Then the sample is injected and capture of any analyte to the sensor chip surface is given as the SPR signal. The bulk RI shift (Δ(II-I) of Figure 1c) can be then correlated to the number of molecules adsorbed onto the surface by comparison with a calibration curve. Association and dissociation kinetics of the molecular interaction can be obtained from the slopes of the injection and dissociation curves. Observation of the SPR sensorgram allows real-time, rapid detection of biomolecular interactions.

1.2 Use of hydrogels for SPR biosensing

Even though SPR sensors are capable of label-free and rapid analysis[8] of biomolecular interactions, they are incapable of distinguishing specific and nonspecific interactions since any adsorption on the sensor surface cause a change in refractive index.[7,9] In addition, conventional SPR biosensors are incapable of detecting small changes in the effective refractive index, especially at ultralow concentrations.[4,10-12] Hence, modification of the SPR sensor to reduce false positives caused by nonspecific interactions and to increase the sensitivity of the SPR response is vital. Studies have been conducted to improve SPR biosensors by developing methods to subtract

nonspecific binding signals[9] or by modifying the sensor surfaces to reduce nonspecific binding[13-18] and increase ligand loading amounts.[19,20]

Modification of the sensor chips with functionalized hydrogels is a promising method to create SPR biosensors with increased specificity and intensity. Hydrogels are three-dimensional crosslinked polymer networks[21.22] with high water content. They can be easily tuned to detect various stimuli via changes in their chemical and physical properties or via immobilization of stimuli responsive receptors onto their surfaces.[23,24] The unique sol-gel transition and swelling-deswelling properties of hydrogels in presence of stimuli make them attractive materials for biosensing.[25]

In terms of SPR biosensing, hydrogels can be used as a support matrix for the attachment of large amounts of ligands.[26] This allows capture of larger amounts of analyte, subsequently increasing the intensity of SPR signals obtained. The stimuli specific response provided by hydrogels can also be utilized to obtain highly selective biosensors.[18]

In this study, we reported the fabrication of hydrogel-based SPR sensor chips for label-free detection of antibody/antigen interactions. In our approach, we grafted hydrogel nanoparticles to SPR sensor chips. Compared to other hydrogel-based approaches that can only experience 1D deswelling due to usage of spin-coated hydrogels[43,44], our hydrogel-based sensor is expected to show higher responses as the hydrogel nanoparticles can deswell

in both the parallel and perpendicular direction. With use of our SPR sensor chips, we were able to investigate the effects of different parameters such as size and crosslinking density on the SPR signal enhancement effect afforded by the hydrogels. From our results, we were able to confirm that tuning of hydrogel properties allows sensing of analytes at different concentrations. Our hydrogel-based sensor shows promise as a tunable biosensor for sensing of various biomarkers and tuning can be easily done by incorporation of different biosensing moieties or by tuning hydrogel properties.

Chapter 2. Experimental Methods

2.1 Materials

All chemical compounds were used without further purification unless otherwise stated. N-isopropylacrylamide (NIPAM, 98%) was purchased from Tokyo Chemical Industry (Tokyo, Japan). Acrylic acid (AAc), *N,N'*-methylenebisacrylamide (BIS), ammonium persulfate (APS), sodium dodecyl sulfate (SDS), poly(oxyethylene) sorbitan monooleate (Tween 80) and *N*-hydroxysuccinimide (NHS) were purchased from Sigma-Aldrich (St. Louis, MO, USA). 1-Ethyl-3-(3-dimethylaminopropyl)carbodiimide (EDC) and 2-(*N*-morpholino)ethanesulfonic acid (MES) buffer was purchased from Thermo Fisher Scientific (Waltham, MA, USA). Dulbecco's phosphate-buffered saline (D-PBS, 1X) was purchased from Welgene (Gyeongsan, Korea). PD-1 protein and PD-1 IgG antibodies were purchased from Sino Biological Inc. (Beijing, P.R.China).

NIPAM was recrystallized from *n*-hexane and dried under vacuum for 4 h prior to use. The water used throughout this entire study was distilled and deionized to 18.2 MΩ cm with an aquaMAX-Ultra 350 water purification system (Young In, Anyang, Korea). The deionized water was filtered with a 0.22 μm filter to remove any particulate matter.

2.2 Hydrogel synthesis

All hydrogels in this study were synthesized via aqueous free-radical precipitation polymerization as reported previously.[18] A total monomer concentration of 70 mM was used for SDS hydrogels while a total monomer concentration of 100 mM was used for Tween 80 hydrogels. The reactants feed used in the synthesis of the hydrogels are summarized in Tables 1 and 2.

In a typical synthesis, 50 mL of reaction mixture was prepared by dissolving NIPAM and BIS in deionized water, followed by addition of surfactant (SDS or Tween 80). The reaction mixture was then filtered with a 0.22 μm syringe-driven filter and transferred to a 100 mL three-neck round-bottomed flask equipped with a reflux condenser, a magnetic stirring bar and a thermometer. The solution was heated to the desired reaction temperature while degassing with Ar gas and stirring at 275 rpm. After 1 h, AAc was added to the flask and Ar purging was maintained for 15 min before addition of 0.2 mL of APS to initiate polymerization. Polymerization was allowed to proceed for 6 h under a constant flow of Ar gas. After synthesis, the mixture was allowed to cool before purification by dialysis (Spectra/Por Float-A-Lyzer G2, MWCO 100 kDa, Repligen, Boston, MA, USA) against deionized water for 2 weeks, with the water changed daily. After purification, the

hydrogels were lyophilized with a TFD8501 freeze dryer (ilShinBioBase, Dongducheon, Korea).

Table 1. Summary of polymerization recipes used for the synthesis of SDS hydrogels. The total monomer concentration was held constant at 70 mM and the AAc concentration was fixed at 7 mM, corresponding to 10% of the total monomer concentration. All synthesis was performed with 1 mM of SDS as surfactant and 2 mM of APS as initiator.

Sample	Reaction	NIPAM	BIS	[APS],
S-BIS2-75	75 °C	88%	2%	2
S-BIS2-70	70 °C	88%	2%	2
S-BIS2-60	60 °C	88%	2%	2
S-BIS4-70	70 °C	86%	4%	2
S-BIS4-60	60 °C	86%	4%	2
S-BIS8-70	70 °C	82%	8%	2
S-BIS8-60	60 °C	82%	8%	2
S-BIS16-70	70 °C	74%	16%	2
S-BIS16-60	60 °C	74%	16%	2

Table 2. Summary of polymerization recipes used for the synthesis of Tween 80 hydrogels. The total monomer concentration was held constant at 100 mM and the AAc concentration was fixed at 10 mM, corresponding to 10% of the total monomer concentration. All synthesis was performed with 0.5 mM of Tween 80 as surfactant.

Sample	Reaction	NIPAM	BIS	[APS],
T-BIS2-70	70 °C	88%	2%	2
T-BIS2-60	60 °C	88%	2%	2
T-BIS2-60-APS1	60 °C	88%	2%	1
T-BIS4-70	70 °C	86%	4%	2
T-BIS4-60	60 °C	86%	4%	2
T-BIS8-70	70 °C	82%	8%	2
T-BIS8-60	60 °C	82%	8%	2
T-BIS8-60-APS1	60 °C	82%	8%	1
T-BIS16-70	70 °C	74%	16%	2
T-BIS16-60	60 °C	74%	16%	2
T-BIS16-60-APS1	60 °C	74%	16%	1

2.3 Characterization of prepared hydrogels

^{1}H NMR spectra were recorded on a Bruker Avance III 400 MHz spectrometer (Billerica, MA, USA), with DMSO-d_6 as solvent. The hydrodynamic diameters and ζ-potential of the hydrogels were measured with a Zetasizer Nano ZS (Malvern Instruments, Worchestershire, UK) equipped with a 633 nm He-Ne laser, and measurements were taken at a 173° detection angle. ζ-Potential measurements were performed with disposable folded capillary cells. The hydrodynamic diameters were acquired through dynamic light scattering (DLS) measurements, with use of disposable polystyrene cuvettes. Size or ζ-potential measurements were conducted after the samples were equilibrated for 2 min at 25 °C. All size or ζ-potential data reported in this study were averaged from 15 individual measurements with 10 s integration time for each measurement.

2.4 PD-1 receptor conjugation to hydrogels

PD-1 functionalization of the hydrogels were conducted by EDC/NHS coupling of the amine groups of the PD-1 receptor molecules to the carboxyl groups of the hydrogels. Typically, the lyophilized hydrogels were suspended in MES buffer (pH 5.6, 100 mM) at a concentration of 10 mg/mL, followed by addition of 10 μL of EDC (0.1 M) and 10 μL of NHS (0.34 M) and

incubated for 5 min at RT. The PD-1 receptor solution was added to the hydrogel mixture to give a final concentration of 0.5 μM and incubated for 1 h at RT. For removal of unreacted EDC, NHS and receptor molecules, the hydrogel mixture was centrifuged 5 times, followed by resuspension in D-PBS buffer. The PD-1 conjugated hydrogels were stored at 4 °C and used the next day.

2.5 Analyte detection through SPR analysis

Sensor chip modification and SPR analysis were conducted at 25 °C in a Biacore T200 apparatus (Cytiva, Malborough, MA, USA), at a constant flow rate of 2 μL/min. Prior to all SPR analysis, untreated gold sensor chips were modified by cysteamine functionalization, followed by grafting of hydrogels onto chip surfaces. Water served as the running buffer for cysteamine functionalization while 0.1 M MES buffer (0.9% sodium chloride, pH 5.6) served as the running buffer for the hydrogel grafting process. The sensor chip surface was activated by flowing 10 mM cysteamine for 600 s. Next, the activated sensor chips were modified with five 60 s flow cycles of hydrogel solution (0.2X in MES buffer), with 120 s in between each cycle.

Analytes (PD-1 Ab solution) were prepared by serial dilution in D-PBS to desired concentrations. Each sensing cycle began with equilibration of the

sensor chip with D-PBS, followed by 60 s injection of the analyte solution, and then 150 s of washing with D-PBS to remove non-specifically bound species. The resulting sensorgrams were analyzed by global fitting using an appropriate model in the Biacore Evaluation Program v2.0.

Chapter 3. Results and Discussion

3.1 Precipitation polymerization of hydrogels

The poly(*N*-isopropylacrylamide-*co*-acrylic acid) (p(NIPAM-*co*-AAc)) hydrogels utilized in this study were synthesized by aqueous free-radical precipitation polymerization as shown in the scheme (Figure 2). Various parameters such as crosslinking density, polymerization temperature, type of surfactant used, and initiator concentration were controlled to synthesize a range of hydrogels of different physical properties. The effects of these parameters will be discussed later in this chapter.

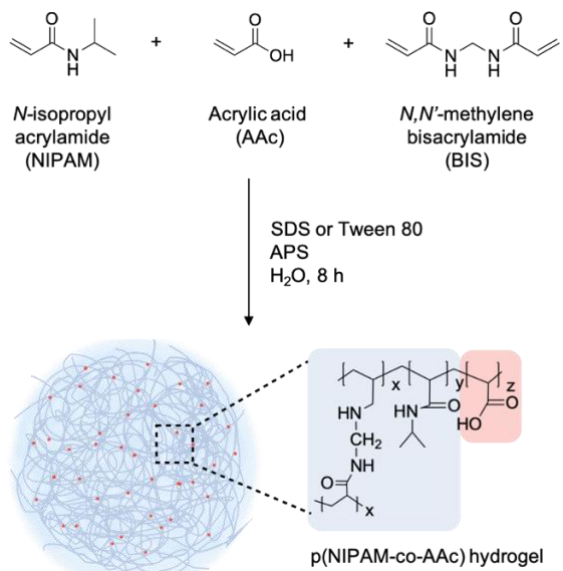

Figure 2. Polymerization scheme used to generate the p(NIPAM-co-AAc) hydrogels used in this study.

The monomers, comprising of *N*-isopropylacrylamide (NIPAM), acrylic acid (AAc) and *N,N'*-methylenebisacrylamide (BIS), were held at total concentrations of 70 mM and 100 mM for SDS and Tween 80 hydrogels, respectively. The molar ratio of AAc was fixed at 10% of the total monomer concentration while the NIPAM and BIS ratio were adjusted accordingly. The exact molar ratios of NIPAM: AAc: BIS for the hydrogels is summarized in Tables 1 and 2, which can be found in Chapter 2 of this work.

AAc was utilized as a comonomer as it imparts carboxyl groups onto the surface of the hydrogels, allowing attachment of receptors through amide-conjugation chemistry. Ammonium persulfate (APS), which decomposes into sulfate anion radicals upon heating, was used to initiate polymerization. Anionic sodium dodecyl sulfate (SDS) or nonionic poly(oxyethylene) sorbitan monooleate (Tween 80) were used as the surfactant.

pNIPAM is thermosensitive polymer with both hydrophobic and hydrophilic moieties in its' repeating unit. It has been widely reported that pNIPAM-based hydrogels undergo coil to globule transitions around its' lower critical solution temperature (LCST) of 32°C due to differences in solubility at different temperatures.[27-29] Below the LCST, hydrogen bonding between water and the amide groups NIPAM allow pNIPAM chains to exist as coils. On the other hand, increasing the temperature above LCST causes

weakening of the hydrogen bonding. Hydrophobic interactions between the polymer backbone and the isopropyl groups become dominant, leading to a preference for the collapsed globular state.

The thermoresponsive properties of pNIPAM can be utilized in the synthesis of pNIPAM-based hydrogels by precipitation polymerization and a schematic depiction of the polymerization mechanism is described in Figure 3.

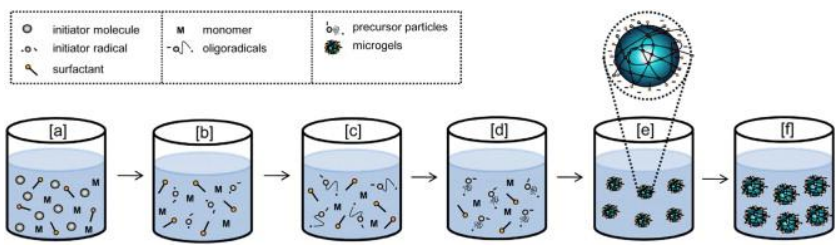

Figure 3. Schematic illustration of the precipitation polymerization process of hydrogels. (a) Homogeneous mixture of reactants, (b) generation of initiator radicals by thermal decomposition of initiator, (c) generation of oligoradicals, (d) generation of precursor particles, (e) growing particles during polymerization, (f) hydrogel mixture at the end of polymerization. Figure is adopted from reference.[30]

Polymerization starts with the heating of a homogeneous mixture of the monomers, surfactant and initiator to temperatures above the LCST of NIPAM. Thermal decomposition of ammonium persulfate (APS) into sulfate

anion radicals initiate polymerization by radical attack on the double bonds of the monomers, generating oligoradicals that act as nucleation sites. Monomers continuously add to the oligoradicals to generate precursor particles. The precursor particles precipitate when the length of the pNIPAM-based backbone reaches a point at which hydrophobic interactions dominate. Nucleation of the precipitated growing particles continue until all of the monomers in the reaction mixture are used up and hydrogels are formed at the end of polymerization.

3.2 Characterization of hydrogels

The successful polymerization of the hydrogels were confirmed through ^{1}H NMR spectroscopy. A comparison between the NMR spectra of the NIPAM monomer and the 2% BIS p(NIPAM-*co*-AAc) hydrogels (Figure 4) shows the disappearance of the double bond protons (b' and c') of the NIPAM monomer. This indicates successful polymerization of the monomers as radical attack results in the consumption of these double bonds in the process of forming the polymer backbone. Peaks ascribed to the NIPAM and AAc comonomers were observed and assigned accordingly in Figure 4(b). Since only a small amount of BIS (2%) was present in the hydrogel sample analyzed by NMR spectroscopy, peaks associated with BIS were not observed.

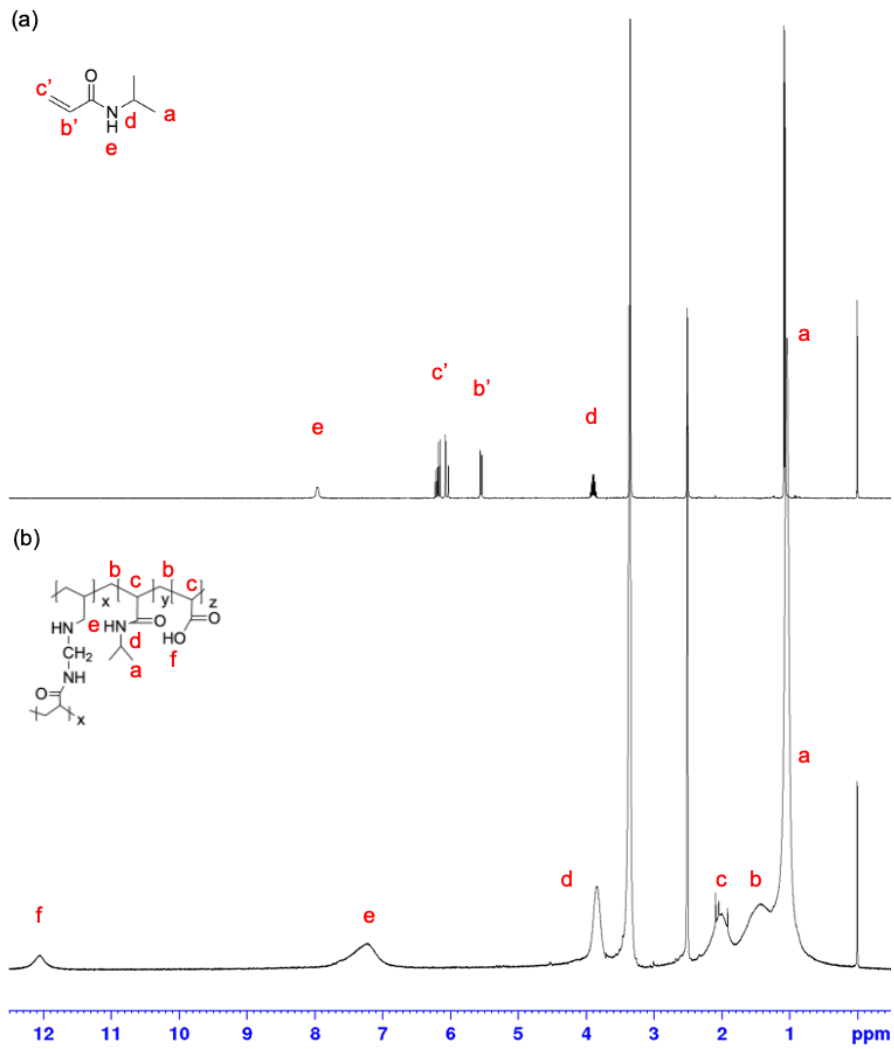

Figure 4. ^{1}H NMR spectra for (a) NIPAM monomer (b) p(NIPAM-co-AAc) hydrogels with 2% BIS content.

The surface charges of the hydrogels were determined through ζ-potential measurements, which is obtained from measurement of the electrophoretic mobility of the sample.[31] All of the hydrogel samples in our

study showed negative ζ-potentials before bioconjugation, indicating the presence of the carboxyl groups on the surface of the hydrogels.

In order to determine the particle size and size distribution of the synthesized hydrogel particles, dynamic light scattering (DLS) studies were conducted. DLS measures the rate of change in intensity of light scattered by particles undergoing Brownian motion in solution.[32-34] The rate at which the scattered light intensity fluctuates is related to the translational diffusion coefficient (D) of the particles, which is then related to the hydrodynamic radius (R_h) of the particles.

The relationship between D and R_h of spherical particles is given by the Stokes-Einstein relationship

$$D = \frac{kT}{6\pi\eta R_h}$$

where k is the Boltzmann's constant, η is the viscosity of the solvent, and T is the absolute temperature. The distribution of D in a sample then gives a distribution of the sizes of particles available.

We were able to synthesize hydrogels with sizes ranging from around 300 nm to 1 μm. The polydispersity (PDI) index of all the synthesized hydrogels below 0.2, indicating highly monodisperse samples.

3.3 Influence of crosslinker concentration on hydrogel size

In order to investigate the effect of crosslinker concentration on size, hydrogels were synthesized at BIS concentrations of 2%, 4%, 8% and 16%. The two double bonds in BIS can be attacked during polymerization to form crosslinks between polymer chains, resulting in 3D hydrogel networks. With increasing BIS concentrations, the average molecular weight and distance between crosslinking points decrease.[35,36] The increased density and reduced mesh sizes cause a decrease in water uptake by the hydrogels, resulting in less swollen structures. The decrease in hydrogel size with increase in crosslinking density is presented in Table 3, Table 4 and Figure 5.

Table 3. Summary of experimental results for SDS hydrogels synthesized with varying crosslinker concentrations. Samples are denoted as S-BISx-70, where x gives the percentage concentration of BIS.

Sample	BIS	D_h (nm)
S-BIS2-70	2%	432.7 ± 66.4
S-BIS4-70	4%	371.6 ± 81.8
S-BIS8-70	8%	306.3 ± 27.6
S-BIS16-70	16%	274.0 ± 82.8

Table 4. Summary of experimental results for Tween 80 hydrogels synthesized with varying crosslinker concentrations. Samples are denoted as T-BISx-70, where x gives the percentage concentration of BIS.

Sample	BIS	D_h (nm)
T-BIS2-70	2%	677.3 ± 98.0
T-BIS4-70	4%	613.9 ± 42.6
T-BIS8-70	8%	585.5 ± 22.3
T-BIS16-70	16%	533.1 ± 16.6

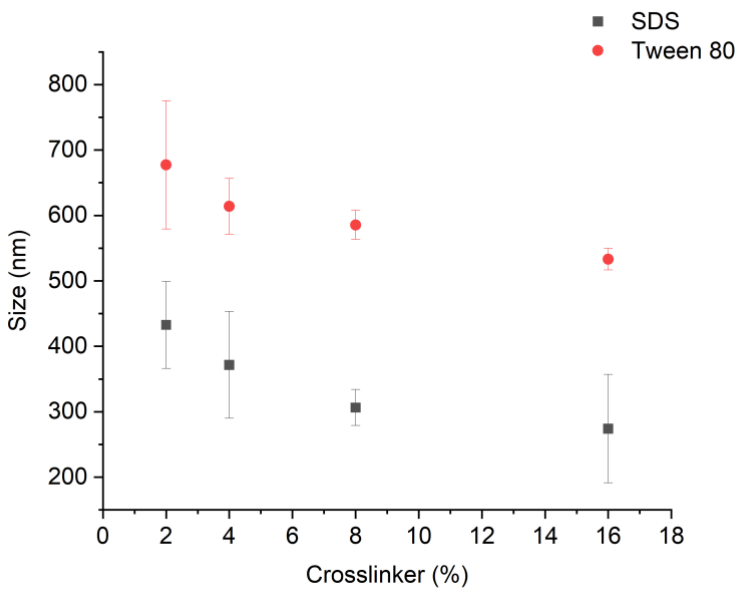

Figure 5. Hydrodynamic sizes of SDS (black squares) and Tween 80 (red circles) hydrogels at different crosslinker densities, as determined by DLS.

3.4 Influence of surfactant on hydrogel synthesis

Surfactants are amphiphilic organic compounds, comprised of hydrophobic tails and hydrophilic heads. They have been reported to reduce interfacial tension during the nucleation phase of aqueous polymerization[37], allowing particles to grow without extensive aggregation. The abilities to stabilize the growing nuclei differ for ionic and nonionic surfactants.

In this study, we utilized SDS as the anionic surfactant, and Tween 80 as the nonionic surfactant. As can be seen from Figure 5, when hydrogels were synthesized at the same reaction conditions, larger particles were obtained when Tween 80 was used. This result indicates that Tween 80 is less effective than SDS at stabilizing the growing polymer nuclei, causing them to be more prone to aggregation, resulting in the formation of larger hydrogel particles.

The weaker stabilizing ability of Tween 80 can be attributed to its' structure. Since their headgroups are nonionic, they experience weaker repulsion between headgroups and associate weakly with polymers.[38] In contrast, the repulsion between the negatively charged heads of SDS promotes hydrophobic interaction between the carbon atoms near the head group. The anionic headgroups in SDS also form stronger electrostatic interactions with the aqueous solvent, making SDS a more effective surfactant.

3.5 Influence of initiator concentration on hydrogel size

The effect of initiator concentration on particle sizes were investigated by synthesis of hydrogels with two different APS concentrations, 1 mM and 2 mM. Figure 6 and Table 5 show the hydrogel sizes for this investigation. It can be seen that at all crosslinker densities, smaller hydrogels were formed when higher amounts of initiator were used.

When low amounts of APS were used to initiate polymerization, lower amounts of early nuclei will be formed and the number of particles that can be potentially formed decreases. Since the amount of monomer consumed by the growing nuclei is the same, more monomers molecules will add to each nucleus, leading to the formation of larger particles.

Table 5. Summary of experimental results for Tween 80 hydrogels synthesized at APS concentrations of 1 mM or 2 mM. Samples synthesized with 1 mM of APS were labelled with a suffix of -APS1.

Sample	BIS	D_h (nm)
T-BIS2-60	2%	707.6 ± 15.7
T-BIS2-60-APS1	2%	946.8 ± 20.5
T-BIS8-60	8%	607.2 ± 18.0
T-BIS8-60-APS1	8%	807.4 ± 29.8
T-BIS16-60	16%	543.7 ± 45.4
T-BIS16-60-APS1	16%	688.1 ± 39.6

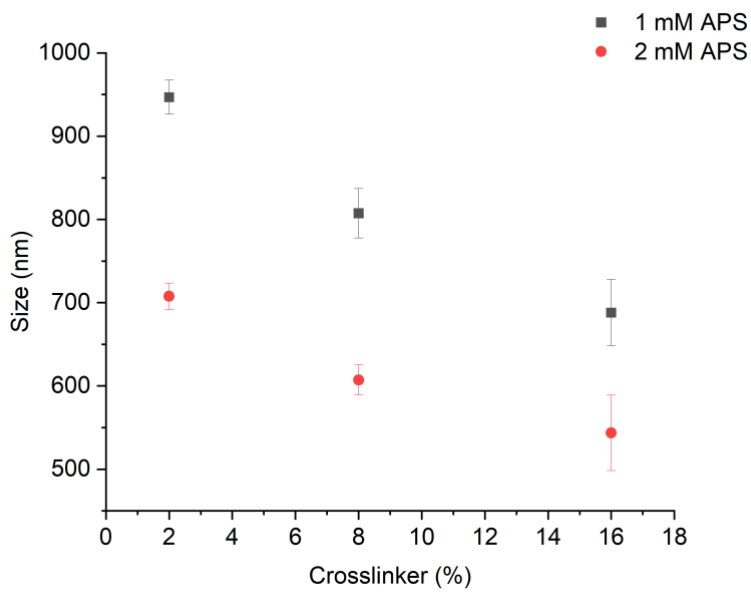

Figure 6. Hydrodynamic sizes of hydrogels synthesized at APS concentrations of 1 mM (black squares) and 2 mM (red circles), as determined by DLS.

3.6 Influence of polymerization temperature on size

It has been previously reported that lower polymerization temperatures give rise to larger hydrogel sizes.[39,40] In our study, the effect of polymerization temperature on hydrogel size was investigated by hydrogel synthesis at 60°C and 70°C.

The results of our study agree with the results suggested in literature, as larger hydrogel particles were obtained for all synthesis conducted at 60°C.

The hydrodynamic diameters of the hydrogels can be found in Table 6, Table 7, Figure 7 and Figure 8.

Table 6. Summary of experimental results for SDS hydrogels synthesized at 60°C or 70°C. Samples were denoted as S-BISx-y, where x gives the crosslinker concentration and y gives the polymerization temperature.

Sample	Reaction temperature	BIS	Size
S-BIS2-70	70°C	2%	432.7 ± 66.5
S-BIS2-60	60°C	2%	611.7 ± 54.2
S-BIS4-70	70°C	4%	371.6 ± 65.4
S-BIS4-60	60°C	4%	451.7 ± 73.3
S-BIS8-70	70°C	8%	306.3 ± 27.6
S-BIS8-60	60°C	8%	378.4 ± 50.6
S-BIS16-70	70°C	16%	202.2 ± 16.5
S-BIS16-60	60°C	16%	257.7 ± 14.8

Table 7. Summary of experimental results for Tween 80 hydrogels synthesized at 60°C or 70°C. Samples were denoted as T-BISx-y, where x gives the crosslinker concentration and y gives the polymerization temperature.

Sample	Reaction	BIS	Size
T-BIS2-70	70°C	2%	649.8 ± 14.4
T-BIS2-60	60°C	2%	707.6 ± 15.7
T-BIS4-70	70°C	4%	613.9 ± 42.6
T-BIS4-60	60°C	4%	684.4 ± 19.9
T-BIS8-70	70°C	8%	585.5 ± 22.3
T-BIS8-60	60°C	8%	607.2 ± 18.0
T-BIS16-70	70°C	16%	533.1 ± 16.6
T-BIS16-60	60°C	16%	543.6 ± 45.4

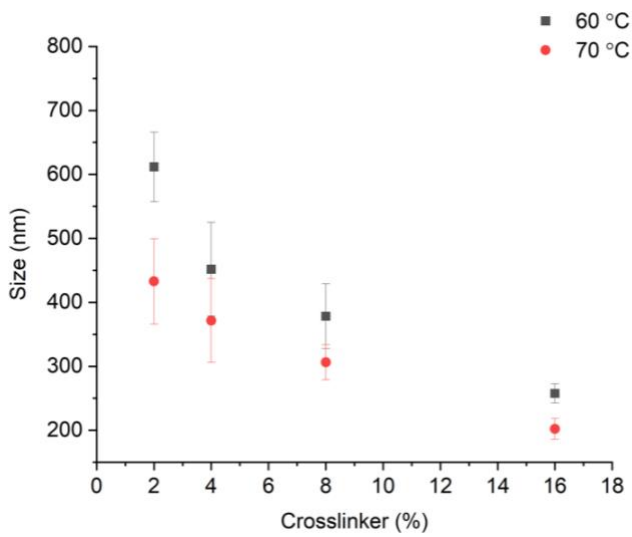

Figure 7. Hydrodynamic sizes of SDS hydrogels synthesized at 60 °C (black squares) and 70 °C (red circles), as determined by DLS.

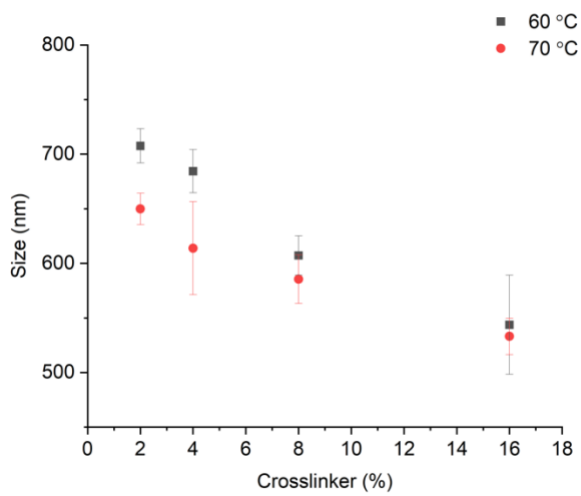

Figure 8. Hydrodynamic sizes of Tween 80 hydrogels synthesized at 60 °C (black squares) and 70 °C (red circles), as determined by DLS.

3.7 SPR sensing of PD-1Ab

Label-free analysis of protein multivalent binding (PMB) to detect antibody/antigen interactions was previously reported by our group.[18] Similar to our previous study, the hydrogels were first modified through EDC/NHS coupling with receptor molecules to impart biosensing abilities. The successful biomodification of the hydrogels can be determined through the slight change in their ζ-potential values.

Introduction of amine groups onto the gold chip surface was conducted by cysteamine-modification of bare gold sensor chips. The negatively charged hydrogels then interact with the positively charged amine groups through charge-charge interactions. This allowed the grafting of the PD-1 receptor functionalized hydrogels onto the gold sensor chip surfaces. The schematic illustration for the fabrication of the SPR sensor chips is depicted in Figure 9 and the change in RU with each process is shown in Figure 10.

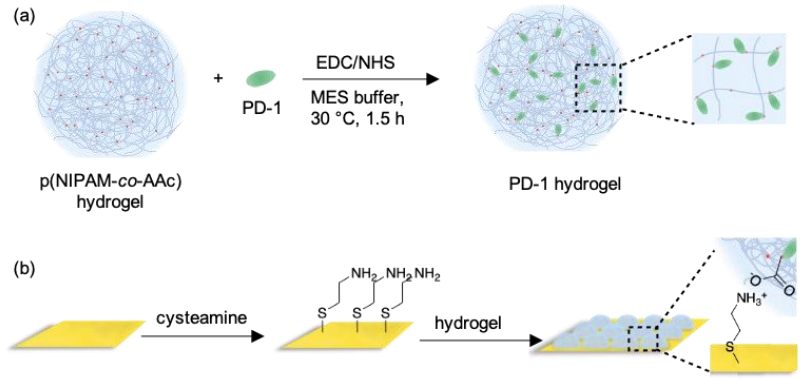

Figure 9. Schematic illustration for the fabrication of the sensor chips. (a) Bioconjugation of the hydrogels with PD-1 receptor through EDC/NHS coupling. (b) Grafting of hydrogels onto bare gold sensor chips.

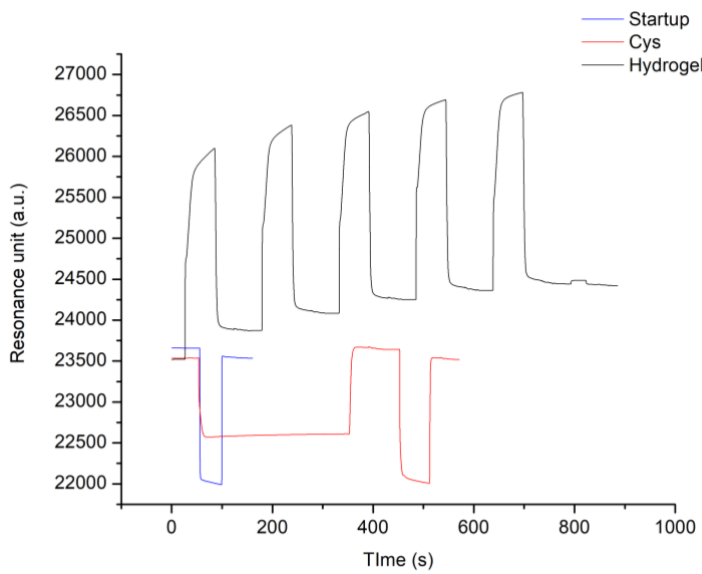

Figure 10. SPR sensorgram depicting the hydrogel grafting process. The chips were first washed with buffer (blue line), modified with cysteamine (red line) and then grafted with hydrogels (black line).

In our study, the interactions between PD-1 receptor modified hydrogels and PD-1 IgG (PD-1Ab) were observed through SPR sensorgrams. When antibody/antigen interactions occur, multivalent binding between two antigen receptors to the Fc region of the IgG antibodies occur. This leads to crosslink formation in the hydrogel network, followed by subsequent deswelling and increase in RI of the hydrogel. Since SPR sensors sense the change in refractive index of the sensor chip surface, stronger SPR signal enhancement effects can be observed when larger RI change occurs.

3.8 Effect of hydrogel size on SPR response

To investigate the relationship between the SPR response and the sizes of hydrogels, sensor chips were grafted with 2% BIS PD-1 hydrogels with varying sizes (Table 8).

Table 8. Summary of the 2% hydrogels before functionalization with PD-1 receptors, as determined by DLS and ζ-potential measurements.

BIS %	Surfactant	Polymerization Temperature	[APS] (mM)	D_h (nm)	PDI	ζ-potential
2%	SDS	75	2	337.1	0.141	-19.8
		70	2	441.0	0.072	-19.7
	Tween 80	70	2	667.7	0.037	-23.4
		60	1	1020	0.150	-11.2

On the other hand, when hydrogels with sizes 400 nm and above were utilized, SNR values above 1 were observed, indicating signal amplification due to PMB.[18] This result suggests that 400 nm is the critical hydrogel size for manifestation of the PMB induced signal enhancement effect.

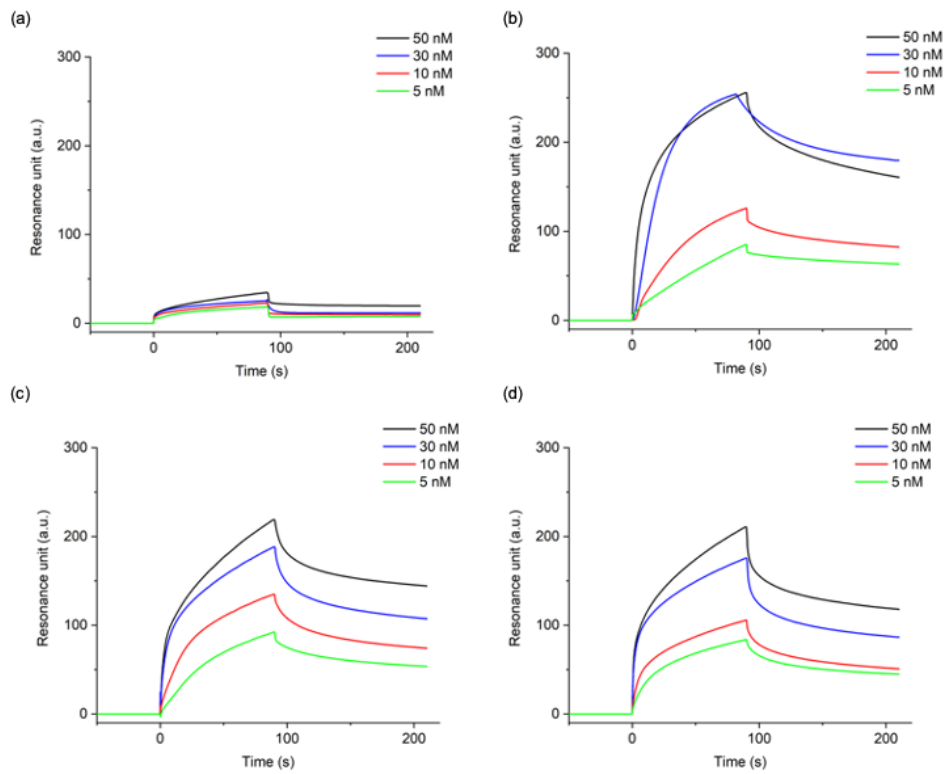

Figure 11. Sensorgrams of sensor chips modified with 2% BIS PD-1 hydrogels of sizes (a) 337 nm (b) 441 nm (c) 668 nm (d) 1020 nm.

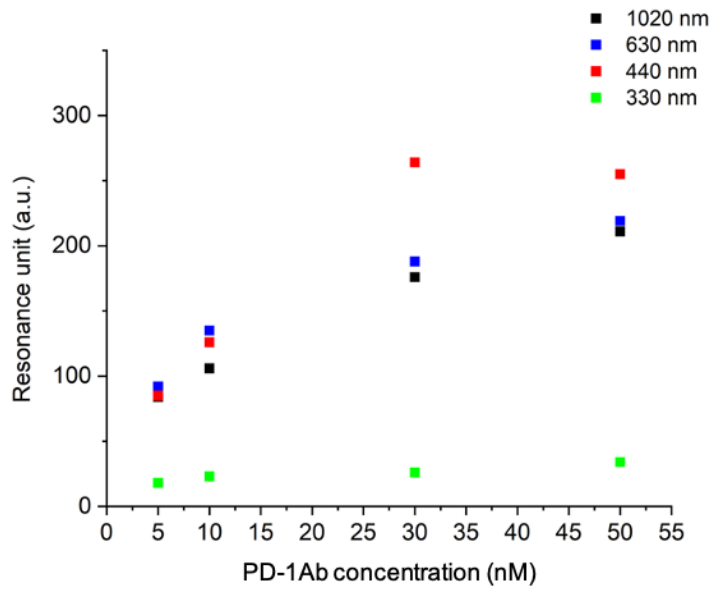

Figure 12. Comparison of the maximum SPR signal of the sensor chips modified with PD-1 hydrogels of different sizes.

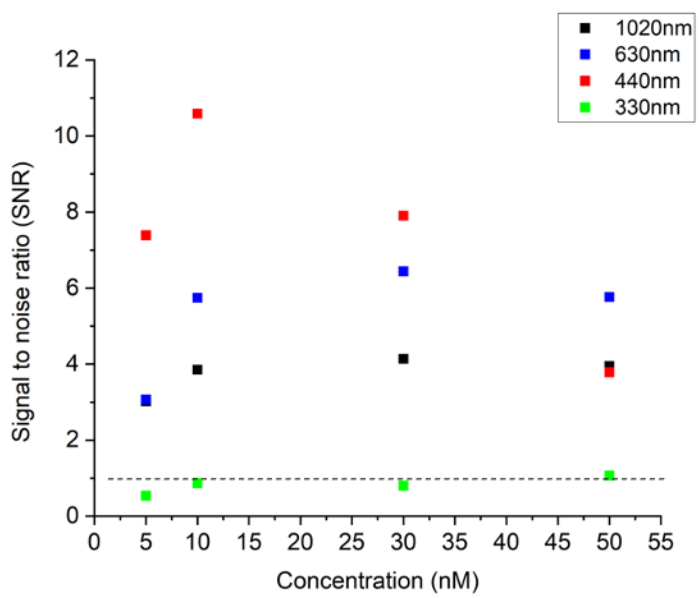

Figure 13. SNR plot of the RUmax values of PD-1 hydrogels against that of unmodified hydrogels.

We postulate that the existence of the critical hydrogel size is caused by the reduction in hydrogel thickness when grafted to planar surfaces.[41] It has been previously reported that grafting of hydrogels causes the particles to be squashed towards the surface in a "pancake-like" morphology. Hence, we can safely assume that hydrogels below 400 nm form a very thin layer over the sensor chip. These hydrogels experience a minimum amount of deswelling in presence of analyte and thus show responses similar to that of unmodified hydrogels.

In contrast, for hydrogels with hydrodynamic sizes above 400 nm, a significantly thick hydrogel layer forms even after the reduction of height caused by grafting. Therefore, in presence of analyte, they experience deswelling and increase in RI, which subsequently leads to amplified SPR signals.

Another interesting point to note is at low concentrations (less than 30 nM), the smaller 440 nm hydrogels showed larger RUmax values compared to the larger 660 nm and 1020 nm hydrogels. However, they exhibited lower RUmax values at 50 nM, suggesting saturation of SPR response of the 440 nm hydrogels at high concentrations. This saturation of response was not observed for the larger hydrogels because the RUmax values for larger hydrogels continue to increase linearly throughout all concentrations tested.

A comparison between the responses of the sensor chips show that smaller hydrogels are more suitable for sensing at low concentrations as they exhibit the highest RUmax values up till the point of saturation, after which their SPR response decreases. On the other hand, larger hydrogels are more appropriate for sensing at high concentrations as they did not show saturation of response at the concentrations tested.

3.9 Effect of crosslinking density on SPR response

The effect of the crosslinking density of the hydrogels on the degree of SPR signal enhancement was also studied. Sensor chips were prepared with similar sized hydrogels crosslinked with 2%, 8% and 16% of BIS (Table 9).

Table 9. Summary of the similarly sized hydrogels before functionalization with PD-1 receptors, as determined by DLS and ζ-potential measurements.

BIS %	Surfactant	Polymerization Temperature	[APS] (mM)	D_h (nm)	PDI	ζ-potential
2%	SDS	70	2	441.0	0.072	-19.7
8%	SDS	60	2	436.5	0.002	-23.0
16%	Tween 80	60	2	522.7	0.003	-24.3

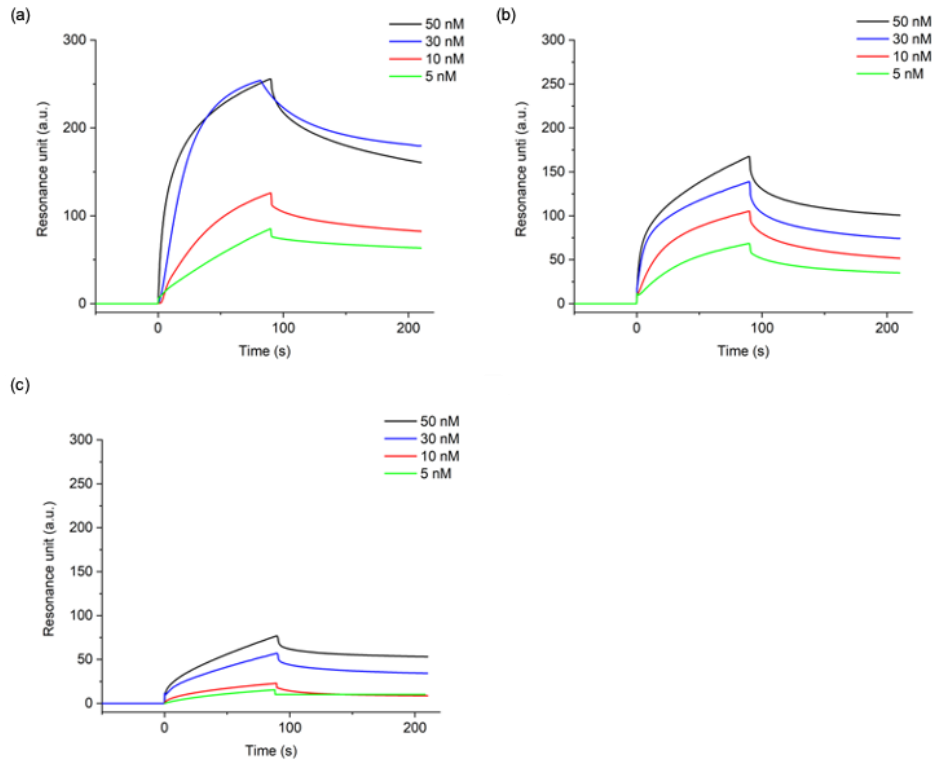

Figure 14. SPR sensorgrams of sensor chips modified with similarly sized PD-1 hydrogels of (a) 2% (b) 8% (c) 16% BIS content.

Similarly, SPR sensorgrams were obtained by in-situ injection of PD-1Ab solutions (Figure 13). From Figure 14, we can see that across all PD-1Ab concentrations tested, increasing crosslinking density decreases the intensity of SPR signal. Hydrogels with higher crosslinking degrees experience less deswelling in the presence of analyte due to their rigid structures. Thus, the difference between the RI of the highly crosslinked

hydrogels in the presence and absence of analytes is less pronounced, resulting in lower SPR signal intensities.

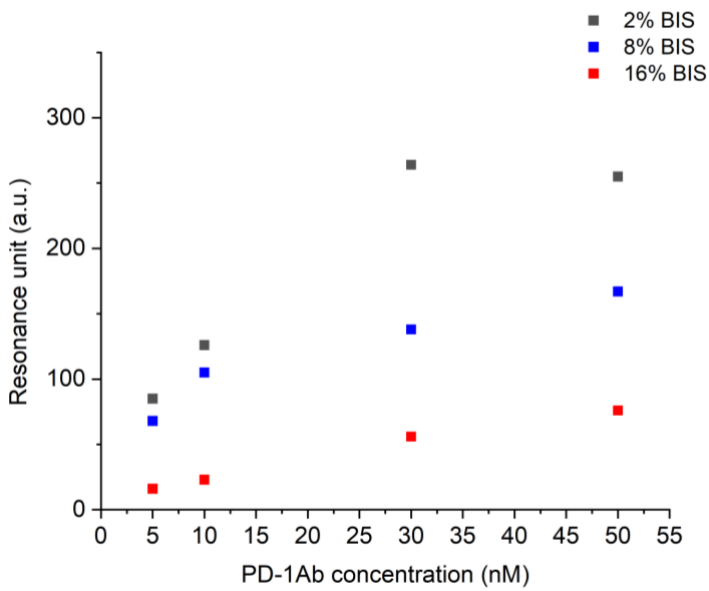

Figure 15. Comparison between the maximum SPR signals of the sensor chips modified with PD-1 hydrogels of different crosslinking degrees.

The SPR signals obtained from tuning the crosslinking degree of hydrogels suggest the possibility of creating hydrogels that are less sensitive but saturate at much higher concentrations. This will make it possible for us to create hydrogel-based SPR sensors that are capable of sensing at different concentration ranges.

Chapter 4. Conclusion

In this report, a label-free biosensor for detection of antibody/antigen interaction was fabricated by the grafting of biofunctionalized hydrogels onto a SPR sensor chip. The hydrogels were first synthesized by aqueous free-radical precipitation polymerization, followed by bioconjugation of receptors through amine-coupling chemistry.

Influence of different parameters such as crosslinker concentration, type of surfactant used, initiator concentration and polymerization temperature on the size and properties of the hydrogels were investigated. Our study revealed that low crosslinker concentration, low initiator concentration, low reaction temperatures, coupled with the use of Tween 80 as surfactant resulted in the formation of large hydrogels.

Additionally, the dependence of the SPR signal on the size and crosslinking density of the hydrogels were observed. Our results show that less crosslinked hydrogels give higher SPR signal responses and the critical hydrogel size for the manifestation of SPR signal response amplification due to PMB is 400 nm. Furthermore, our results suggest that smaller hydrogels are more sensitive at analyte concentrations below their saturation point while

larger hydrogels are less sensitive but can produce responses at high analyte concentrations.

In conclusion, our results hint at the possibility of engineering hydrogels to produce biosensors with tunable detection ranges. Since clinically relevant concentrations differ from one biomarker to another[42], this finding is especially notable as it hints at the possibility of using the same biosensor system for diagnosis of different diseases.

Bibliography

(1) Im, H.; Lesuffleur, A.; Lindquist, N. C.; Oh, S.-H. Plasmonic Nanoholes in a Multichannel Microarray Format for Parallel Kinetic Assays and Differential Sensing. *Anal. Chem.* **2009**, *81* (8), 2854–2859.

(2) Bolduc, O. R.; Masson, J.-F. Advances in Surface Plasmon Resonance Sensing with Nanoparticles and Thin Films: Nanomaterials, Surface Chemistry, and Hybrid Plasmonic Techniques. *Anal. Chem.* **2011**, *83* (21), 8057–8062.

(3) Arima, Y.; Toda, M.; Iwata, H. Surface Plasmon Resonance in Monitoring of Complement Activation on Biomaterials. *Adv. Drug Deliv. Rev.* **2011**, *63* (12), 988–999.

(4) Qu, J.-H.; Dillen, A.; Saeys, W.; Lammertyn, J.; Spasic, D. Advancements in SPR Biosensing Technology: An Overview of Recent Trends in Smart Layers Design, Multiplexing Concepts, Continuous Monitoring and in Vivo Sensing. *Anal. Chim. Acta* **2020**, *1104*, 10–27.

(5) Zeng, S.; Baillargeat, D.; Ho, H.-P.; Yong, K.-T. Nanomaterials Enhanced Surface Plasmon Resonance for Biological and Chemical Sensing Applications. *Chem. Soc. Rev.* **2014**, *43* (10), 3426–3452.

(6) Homola, J. Surface Plasmon Resonance Sensors for Detection of Chemical and Biological Species. *Chem. Rev.* **2008**, *108* (2), 462–493.

(7) Schasfoort, R. B. M. Chapter 1. Introduction to Surface Plasmon Resonance. In *Handbook of Surface Plasmon Resonance*; Royal Society of Chemistry: Cambridge, 2017; pp 1–26.

(8) Singh, P. SPR Biosensors: Historical Perspectives and Current Challenges. *Sens. Actuators B Chem.* **2016**, *229*, 110–130.

(9) Visentin, J.; Couzi, L.; Dromer, C.; Neau-Cransac, M.; Guidicelli, G.; Veniard, V.; Coniat, K. N.-L.; Merville, P.; Di Primo, C.; Taupin, J.-L. Overcoming Non-Specific Binding to Measure the Active Concentration and Kinetics of Serum Anti-HLA Antibodies by Surface Plasmon Resonance. *Biosens. Bioelectron.* **2018**, *117*, 191–200.

(10) Chang, Y.-F.; Wang, W.-H.; Hong, Y.-W.; Yuan, R.-Y.; Chen, K.-H.; Huang, Y.-W.; Lu, P.-L.; Chen, Y.-H.; Chen, Y.-M. A.; Su, L.-C.; Wang, S.-F. Simple Strategy for Rapid and Sensitive Detection of Avian Influenza A H7N9 Virus Based on Intensity-Modulated SPR Biosensor and New Generated Antibody. *Anal. Chem.* **2018**, *90* (3), 1861–1869.

(11) He, L.; Musick, M. D.; Nicewarner, S. R.; Salinas, F. G.; Benkovic, S. J.; Natan, M. J.; Keating, C. D. Colloidal Au-Enhanced Surface

Plasmon Resonance for Ultrasensitive Detection of DNA Hybridization. *J. Am. Chem. Soc.* **2000**, *122* (38), 9071–9077.

(12) Su, L.-C.; Chang, C.-M.; Tseng, Y.-L.; Chang, Y.-F.; Li, Y.-C.; Chang, Y.-S.; Chou, C. Rapid and Highly Sensitive Method for Influenza A (H1N1) Virus Detection. *Anal. Chem.* **2012**, *84* (9), 3914–3920.

(13) Masson, J.-F.; Battaglia, T. M.; Cramer, J.; Beaudoin, S.; Sierks, M.; Booksh, K. S. Reduction of Nonspecific Protein Binding on Surface Plasmon Resonance Biosensors. *Anal. Bioanal. Chem.* **2006**, *386* (7–8), 1951–1959.

(14) Chou, Y.-N.; Sun, F.; Hung, H.-C.; Jain, P.; Sinclair, A.; Zhang, P.; Bai, T.; Chang, Y.; Wen, T.-C.; Yu, Q.; Jiang, S. Ultra-Low Fouling and High Antibody Loading Zwitterionic Hydrogel Coatings for Sensing and Detection in Complex Media. *Acta Biomater.* **2016**, *40*, 31–37.

(15) Li, J.; Ji, C.; Yu, X.; Yin, M.; Kuckling, D. Dually Cross-Linked Supramolecular Hydrogel as Surface Plasmon Resonance Sensor for Small Molecule Detection. *Macromol. Rapid Commun.* **2019**, *40* (14), e1900189.

(16) Li, J.; Ji, C.; Lü, B.; Rodin, M.; Paradies, J.; Yin, M.; Kuckling, D. Dually Crosslinked Supramolecular Hydrogel for Cancer Biomarker Sensing. *ACS Appl. Mater. Interfaces* **2020**, *12* (33), 36873–36881.

(17) Naraprawatphong, R.; Kawamura, A.; Miyata, T. Preparation of Molecularly Imprinted Hydrogel Layer SPR Sensor Chips with Lectin-Recognition Sites via SI-ATRP. *Polym. J.* **2018**, *50* (3), 261–269.

(18) Yang, H. M.; Teoh, J. Y.; Yim, G. H.; Park, Y.; Kim, Y. G.; Kim, J.; Yoo, D. Label-Free Analysis of Multivalent Protein Binding Using Bioresponsive Nanogels and Surface Plasmon Resonance (SPR). *ACS Appl. Mater. Interfaces* **2020**, *12* (5), 5413–5419.

(19) Li, J.; Yu, X.; Herberg, A.; Kuckling, D. Biomolecule Sensor Based on Azlactone-Modified Hydrogel Films. *Macromol. Rapid Commun.* **2019**, *40* (7), e1800674.

(20) Sato, Y.; Ikegaki, S.; Suzuki, K.; Kawaguchi, H. Hydrogel-Microsphere-Enhanced Surface Plasmon Resonance for the Detection of a K-Ras Point Mutation Employing Peptide Nucleic Acid. *J. Biomater. Sci. Polym. Ed.* **2003**, *14* (8), 803–820.

(21) Oh, K. S.; Oh, J. S.; Choi, H. S.; Bae, Y. C. Effect of Cross-Linking Density on Swelling Behavior of NIPA Gel Particles. *Macromolecules* **1998**, *31* (21), 7328–7335.

(22) Li, J.; Mooney, D. J. Designing Hydrogels for Controlled Drug Delivery. *Nat. Rev. Mater.* **2016**, *1* (12), 16071.

(23) Ahmed, E. M. Hydrogel: Preparation, Characterization, and Applications: A Review. *J. Adv. Res.* **2015**, *6* (2), 105–121.

(24) Tavakoli, J.; Tang, Y. Hydrogel Based Sensors for Biomedical Applications: An Updated Review. *Polymers (Basel)* **2017**, *9* (8), 364.

(25) Jung, I. Y.; Kim, J. S.; Choi, B. R.; Lee, K.; Lee, H. Hydrogel Based Biosensors for in Vitro Diagnostics of Biochemicals, Proteins, and Genes. *Adv. Healthc. Mater.* **2017**, *6* (12), 1601475.

(26) Mateescu, A.; Wang, Y.; Dostalek, J.; Jonas, U. Thin Hydrogel Films for Optical Biosensor Applications. *Membranes (Basel)* **2012**, *2* (1), 40–69.

(27) Deen, G. R.; Alsted, T.; Richtering, W.; Pedersen, J. S. Synthesis and Characterization of Nanogels of Poly(*N*-Isopropylacrylamide) by a Combination of Light and Small-Angle X-Ray Scattering. *Phys. Chem. Chem. Phys.* **2011**, *13* (8), 3108–3114.

(28) Arleth, L.; Xia, X.; Hjelm, R. P.; Wu, J.; Hu, Z. Volume Transition and Internal Structures of Small Poly(*N*-Isopropylacrylamide) Microgels. *J. Polym. Sci. B Polym. Phys.* **2005**, *43* (7), 849–860.

(29) Jain, K.; Vedarajan, R.; Watanabe, M.; Ishikiriyama, M.; Matsumi, N. Tunable LCST Behavior of Poly(*N*-Isopropylacrylamide/Ionic Liquid) Copolymers. *Polym. Chem.* **2015**, *6* (38), 6819–6825.

(30) von Nessen, K.; Karg, M.; Hellweg, T. Thermoresponsive Poly-(*N*-Isopropylmethacrylamide) Microgels: Tailoring Particle Size by Interfacial Tension Control. *Polymer (Guildf.)* **2013**, *54* (21), 5499–5510.

(31) Předota, M.; Machesky, M. L.; Wesolowski, D. J. Molecular Origins of the Zeta Potential. *Langmuir* **2016**, *32* (40), 10189–10198.

(32) Hassan, P. A.; Rana, S.; Verma, G. Making Sense of Brownian Motion: Colloid Characterization by Dynamic Light Scattering. *Langmuir* **2015**, *31* (1), 3–12.

(33) Shang, J.; Gao, X. Nanoparticle Counting: Towards Accurate Determination of the Molar Concentration. *Chem. Soc. Rev.* **2014**, *43* (21), 7267–7278.

(34) Liu, X.; Dai, Q.; Austin, L.; Coutts, J.; Knowles, G.; Zou, J.; Chen, H.; Huo, Q. A One-Step Homogeneous Immunoassay for Cancer Biomarker Detection Using Gold Nanoparticle Probes Coupled with Dynamic Light Scattering. *J. Am. Chem. Soc.* **2008**, *130* (9), 2780–2782.

(35) Zhang, H.; Huang, X.; Jiang, J.; Shang, S.; Song, Z. Hydrogels with High Mechanical Strength Cross-Linked by a Rosin-Based Crosslinking Agent. *RSC Adv.* **2017**, *7* (67), 42541–42548.

(36) Wong, R. S. H.; Ashton, M.; Dodou, K. Effect of Crosslinking Agent Concentration on the Properties of Unmedicated Hydrogels. *Pharmaceutics* **2015**, *7* (3), 305–319.

(37) Meconi, G. M.; Ballard, N.; Asua, J. M.; Zangi, R. Adsorption and Desorption Behavior of Ionic and Nonionic Surfactants on Polymer Surfaces. *Soft Matter* **2016**, *12* (48), 9692–9704.

(38) Robb, I. D.; Stevenson, P. Interaction between Poly(Acrylic Acid) and an Ethoxylated Nonionic Surfactant. *Langmuir* **2000**, *16* (18), 7168–7172.

(39) Meng, Z.; Smith, M. H.; Lyon, L. A. Temperature-Programmed Synthesis of Micron-Sized Multi-Responsive Microgels. *Colloid Polym. Sci.* **2009**, *287* (3), 277–285.

(40) Liu, A. L.; García, A. J. Methods for Generating Hydrogel Particles for Protein Delivery. *Ann. Biomed. Eng.* **2016**, *44* (6), 1946–1958.

(41) Seeber, M.; Zdyrko, B.; Burtovvy, R.; Andrukh, T.; Tsai, C.-C.; Owens, J. R.; Kornev, K. G.; Luzinov, I. Surface Grafting of Thermoresponsive Microgel Nanoparticles. *Soft Matter* **2011**, *7* (21), 9962.

(42) Pongruengkiat, W.; Pechprasarn, S. Whispering-Gallery Mode Resonators for Detecting Cancer. *Sensors (Basel)* **2017**, *17* (9), 2095.

(43) Buller, J.; Laschewsky, A.; Wischerhoff, E. Photoreactive Oligoethylene Glycol Polymers – Versatile Compounds for Surface Modification by Thin Hydrogel Films. *Soft Matter* **2013**, *9* (3), 929–937.

(44) Mateescu, A.; Wang, Y.; Dostalek, J.; Jonas, U. Thin Hydrogel Films for Optical Biosensor Applications. *Membranes (Basel)* **2012**, *2* (1), 40–69.

국문 초록

SPR 바이오 센서는 사전 라벨링이 필요하지 않은 상태에서 실시간으로 이러한 상호 작용을 모니터링할 수 있기 때문에 생체 분자 상호 작용의 탐지 및 진단 분야에 널리 사용되는 진단 키트이다. 하지만 이러한 SPR 바이오 센서는 비특이적 상호 작용과 특정 상호 작용을 구별할 수 없다는 점과 낮은 민감도와 같은 몇 가지 한계점을 가지고 있다.

센서 칩은 SPR 바이오 센서의 가장 중요한 구성 요소 중 하나이며 센서 칩의 특성은 분석 물질의 존재 하에서 센서의 민감도와 특이성을 좌우한다. 바이오 반응성 하이드로젤은 특정 자극에 대한 선택성과 함께 오손 방지 특성을 가지고 있다고 보고된 바가 있어, 하이드로젤의 이식은 SPR 바이오 센서의 특이성을 향상시킬 것으로 기대된다. 겔 매트릭스의 3 차원 구조는 또한 리간드 고정화에 대한 더 많은 부착 부위를 제공하여 바이오 센서의 감도를 향상시킬 수 있다.

본 연구에서는 바이오 반응성 하이드로겔을 이용한 베어 골드 센서 칩의 표면 개질로 바이오 반응성 SPR 센서 칩을 제작하였다. 하이드로겔의 간편한 합성 단계를 통해 우리는 다른 물리적 특성을 가진 하이드로겔 라이브러리를 합성하였다. 또한, 하이드로겔의 물리적 특성이 SPR 반응에 미치는 영향을 조사하였다. 본 연구의 결과는 다양한 농도 범위에서 최적의

감도를 갖는 SPR 바이오센서를 제작하기 위한 하이드로젤의 특성의 가능성을 보여준다.